OPEN ACCESS

Saudi Journal of Engineering and Technology
Abbreviated Key Title: Saudi J Eng Technol
ISSN 2415-6272 (Print) | ISSN 2415-6264 (Online)
Scholars Middle East Publishers, Dubai, United Arab Emirates
Journal homepage: https://saudijournals.com

Original Research Article

Thermal and Structural Modelling of Laboratory-Scale Pyrolysis Reactor

Akinsade, A[1], Akinola, A. O[2*], Yaru, S. S[2], Eiche, J. F[1]

[1]Department of Mechanical Engineering, Olusegun Agagu University of Science and Technology, Okitipupa, Nigeria
[2]Department of Mechanical Engineering, The Federal University of Technology, Akure, Nigeria

DOI: 10.36348/sjet.2024.v09i02.004 | **Received:** 10.12.2023 | **Accepted:** 22.01.2024 | **Published:** 02.02.2024

***Corresponding author:** Akinola, A. O
Department of Mechanical Engineering, The Federal University of Technology, Akure, Nigeria

Abstract

This paper presents the steady-state thermal and static structural modelling of a laboratory-scale pyrolysis reactor for the thermal degradation of biomass wastes. A laboratory-scale pyrolysis reactor of volume 9.203 x $10^{-3}m^3$ was developed to pyrolyse Palm Kernel Shell (PKS) and Palm Fruit Bunch (PFB) at varying temperatures of 350ºC, 400ºC, 450ºC, 500ºC, and 550ºC. The reactor chamber was simulated for static-steady thermal and static structural analysis to determine the temperature distribution and thermal stresses induced in it. The model was developed using SolidWorks software, and a Computational Fluid Dynamics (CFD) simulation was carried out using ANSYS Workbench 19. A total number of 2,459 elements was generated composed of 8630 nodes using Hexahedra dominant meshing method. It was observed from the simulation result that the temperature distribution inside and outside the reactor chamber were 454.29ºC and 550ºC respectively. The maximum heat flux of 8.3466e+005 W/m² occurred at the inner chamber of the reactor due to the high concentration of the biomass waste and devolatization reaction, and the maximum equivalent (von-Mises) stresses the material can withstand at higher temperature is 1.6674e+009 Pa without rupture. It was found out from the simulation result that at a maximum temperature of 550ºC, the equivalent (von Mises) stresses induced at the outer and inner chamber is 1.8585e+008 Pa, which is far lower than the maximum stress the material can withstand without rupture. Thus, the reactor is safe to operate at a temperature higher than 550ºC without failure.

Keywords: Structural modelling, pyrolysis, thermal stresses, laboratory -scale, pyrolysis reactor, thermal degradation.

1. INTRODUCTION

Energy derived from biomass is making a benchmark despite an assortment of sustainable power sources accessible on the earth due to little dependency on geographical location and climate variation, which are proven diversification factors of biomass that can grow in heterogeneous conditions [1]. Biomass is the only other naturally occurring energy-containing carbon resource that is large enough in quantity to be used as a substitute for fossil fuels [2]. Exhaustible fossil fuels are currently burned to meet 85% of the world's energy needs. By 2025, there will likely be a 50% rise in the world's energy consumption, with quickly developing nations accounting for the majority of this growth. The need for a long-term alternative energy supply that is renewable is evident given the expanding world population, rising energy demand per person, and global warming [3]. Renewable energy from biomass is one of the most promising means to resolve the issue of future energy demand since; it is clean and has no negative impact on the environment and the ecosystem [4].

Biomass can be converted to thermal energy, liquid, solid or gaseous fuels, and other chemical products through a variety of conversion processes that have been proposed by many researchers [5-7]. The thermochemical conversion process is the thermal decomposition of the organic components of biomass into biofuel and is produced by applying heat and chemical processes to biomass [8]. The major processes are combustion, torrefaction, liquefaction, gasification, and pyrolysis [9, 10, 8].

Pyrolysis, the thermal decomposition of biomass by heating either in the absence of oxygen or in a limited supply of oxygen, is carried out at 400–800ºC.

The main products are usually referred to as condensable (tars) and non-condensable volatiles and char. The condensable volatiles are often classified as liquids (bio-oils), while the non-condensable volatiles compose gases, mainly CO, CO_2, H_2, ethane, and ethene [11, 12].

The reactor is the heart of the pyrolysis process; it is a place where all reactions occur [13, 14]. Selection of the type of reactor for biomass pyrolysis is important as it has significant effects on the product composition and yields and also, quality predictions are difficult because the dynamics of each pyrolysis reactor are different [15]. Researchers have studied the modelling and optimization of pyrolysis reactors for thermal analysis to predict the behaviour of the reactor during the pyrolysis process. Queseda *et al.*, [16], studied the optimization of the pyrolysis process of plastic waste to obtain a liquid fuel using different mathematical models with optimum operating temperature conditions of 500^{o}C, a residence time of 120mins and a 20^{o}C/min heating rate. Zhang *et al.*, [17], performed a numerical investigation on the heat transfer in a rotary pyrolysis furnace; it was observed the heat transfer rate was increased when the granular heat carriers were loaded on the reactor. In the same vein, Kumar *et al.*, [18], carried out that analysis and simulation of a small-scale pyrolysis reactor modelled using 3D CAD software and evaluated using ANSYS software, for conversion of plastic waste to fuel at temperatures up to 650^{o}C. it was found that the maximum and minimum thermal stress and strain values developed inside the mini reactor were 127MPa, 158MPa, and 0.001529 and 0.001649 respectively. Jhung [19], performed a fatigue analysis of SMART (System-Integrated Modular Advanced Reactor) during arbitrary transients, the results were applied to a finite element model to determine heat transfer coefficients and stress developed, which are used to calculate the cumulative usage factor. The cumulative usage factor was found to be 0.00699 which is well below the allowable level of 1.0. Also, Mellin *et al.*, [20], developed a comprehensive chemistry model for fast pyrolysis in a fluidized bed assuming the biomass decomposition via both primary and secondary reactions. Xue *et al.*, [21], developed a Eulerian-Eulerian model for fast pyrolysis of biomass in a fluidized bed reactor using a multi-kinetic model for biomass reaction and predicted maximum bio-oil production at about 500 which is in good agreement with the experimental results. In the report of [22], numerical modelling was used to simulate biomass pyrolysis in a fixed bed reactor at a heating rate of 1073 kJ/kWh, with temperatures ranging from 523 K to 923 K. Results revealed good agreement between the experimental and numerical results.

In this study, a pyrolysis reactor made from Stainless-Steel SS 316 Grade with the dimensions of 270 mm X 260 mm was developed and modelled using SolidWorks software as shown in Figure 1, to predict the thermal and structural behaviour of the material at high temperatures during the pyrolysis reaction. CFD simulation using ANSYS Workbench 19 was used to simulate the thermal and static structural analysis of the reactor chamber. A 2.0 kW heater band of 272 mm diameter was wrapped around the reactor to serve as a heat source.

2. MATERIAL AND METHODS

2.1 Materials

In this study, an autoclave made of stainless steel was used as the reactor chamber because of the highly corrosive nature of bio-oil and high operating temperature. The piping from the reactor chamber to the condenser is made from stainless steel. The properties of the material used for the reactor chamber are shown in Table 1.

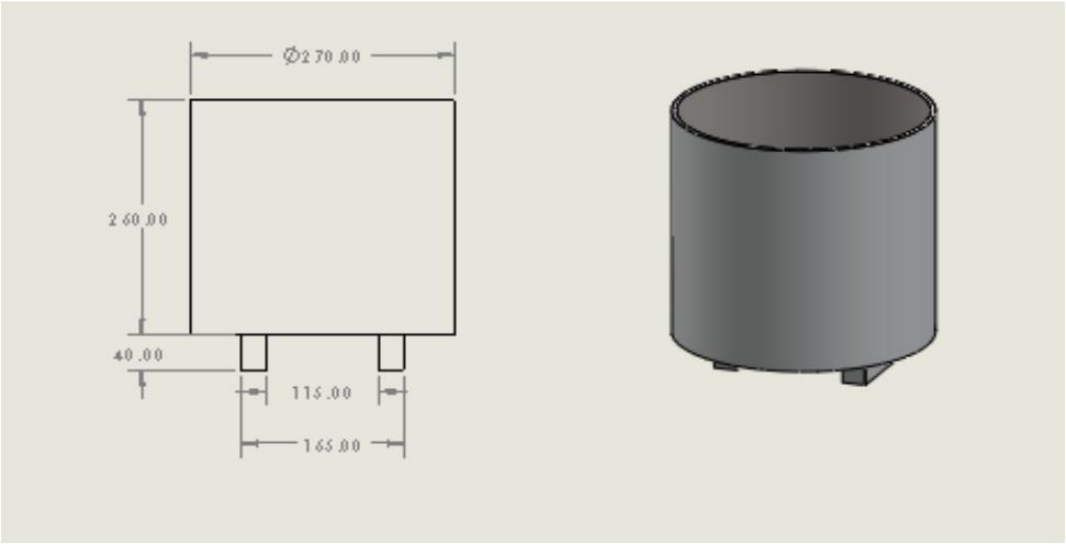

Figure 1: Reactor Chamber Model

Table 1: Properties of Reactor Material

Parameter	Unit	Stainless steel (Ferritic)
Density	kgm^{-3}	7720
Coefficient of Thermal Expansion	K^{-1}	1.05E -005
Poisson's Ratio	-	0.28
Shear modulus	MPa	7.812E + 0.10
Ultimate Tensile Strength	MPa	5.08E +008
Thermal Conductivity	$Wm^{-1}C^{-1}$	24.5
Young Modulus	MPa	2.E + 0.11

2.2 Methods

2.2.1 Heat Transfer Model

The mode of heat transfer (conduction, convection, and radiation) in the solid interface was used to model the heat transfer in the reactor chamber. Temperature and the flow of heat are the basic principles of heat transfer. The heat conduction equations used in this model are given in Equations (1) and (2) [23].

$$\rho c \frac{\partial T}{\partial t} + \rho c_p . \nabla T + \nabla q = Q + Q_{ted} \quad \ldots\ldots\ldots (1)$$

$$q = -k \nabla T \quad \ldots\ldots\ldots\ldots\ldots\ldots\ldots\ldots\ldots\ldots (2)$$

where: ρ is the density, ∂T is the change in Temperature, C_p is the heat capacity at constant pressure, $. \nabla T$ is the temperature gradient, ∇q is the heat flux gradient, Q is the total heat transfer and k is the thermal conductivity.

2.2.2 Reactor Model Equations

CFD model was employed in the modelling of the reactor chamber to simulate the steady-state thermal and static structural analysis using ANSYS Workbench 19. Steady-state thermal analysis is used to determine the temperature distributions and thermal stresses of the reactor model. The analysis was based on the type of material and the diameter of the reactor chamber. Various contours were plotted for the boundary conditions and different paraments were calculated. The air, as working fluid inside the reactor was assumed three-dimensional, in a steady state, compressible, and turbulent. The governing equations are continuity, momentum and energy equations, which apply to the flow from Reynold-average Naiver-stroke equations as given in Equations (3), (4), and (5) [24, 25].

$$\frac{\partial \rho}{\partial t} + \frac{\partial}{\partial x_j}\left(\rho U_j\right) = 0 \quad \ldots\ldots\ldots\ldots\ldots\ldots\ldots\ldots (4)$$

$$\frac{\partial \rho U_i}{\partial t} + \frac{\partial}{\partial t}\left(\rho U_i U_j\right) = -\frac{\partial P}{\partial x_i} + \frac{\partial}{\partial x}\left[\tau_{ij} - \rho U_i U_j\right] \ldots (5)$$

$$\frac{\partial \rho h_t}{\partial t} - \frac{\partial P}{\partial t} + \frac{\partial}{\partial x_j}\left(\rho U_j h_t\right) = -\frac{\partial}{\partial x_i}\left(K \frac{\partial T}{\partial x_i} - \rho \overline{U_j h}\right) + \frac{\partial}{\partial x_j}\left[U_i\left(\tau_{ij} - \rho \overline{U_i U_j}\right)\right] + S_H \quad \ldots\ldots\ldots\ldots\ldots\ldots (6)$$

Where:

ρ is the density, t is the time, U is the directional velocity, p is the pressure, τ is the stress tensor, h_t is the total enthalpy, k is the thermal conductivity, T is the temperature, and S_H is the heat source term. The unknown quantities, namely directional velocity, pressure, and enthalpy, use the average of Reynolds. During this process, the Reynolds stress term ($\overline{U_i U_j}$) and the turbulent flux term ($\rho U_j h_t$) are produced.

2.2.3 Mesh Generation and Boundary Conditions

The geometry of the simulation domain was discretized into finite elements. A total number of 2,459 elements were generated using Hexahedra dominant meshing method composed of 8,630 nodes as shown in Figure 2. The boundary conditions were set based on the designed values as shown in Figure 3.

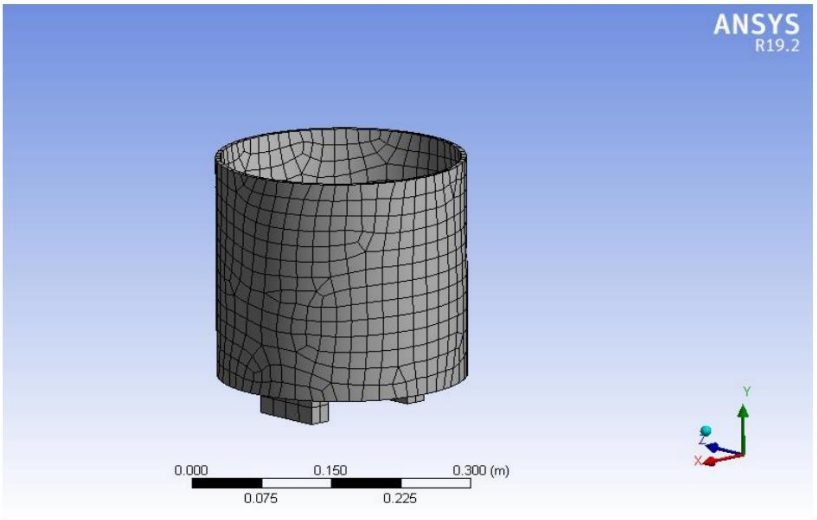

Figure 2: Mesh Generation

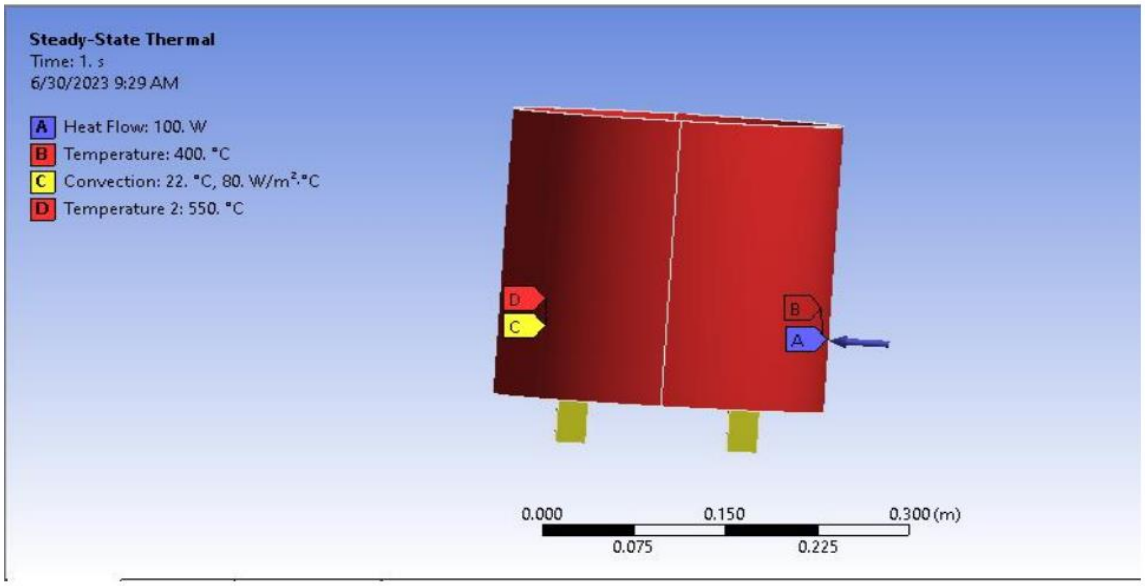

Figure 3: Boundary Conditions

3. RESULT AND DISCUSSION

3.1 Temperature Distribution

Figure 4 shows the temperature distribution along the reactor.

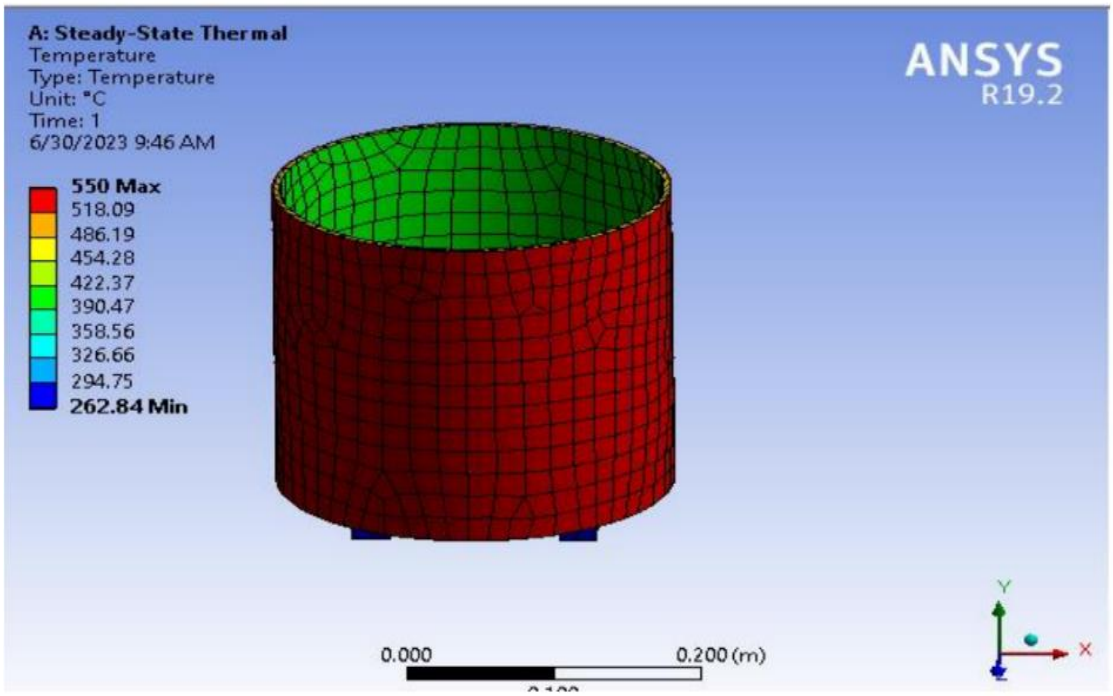

Figure 4: Temperature Distribution

It was observed that maximum temperature occurred at the outer part of the reactor and within the inner part of the reactor where pyrolysis reaction take place, the inside temperature was found out to be 454.28^{o}C and the outer part maximum temperature was 550^{o}C. This shows that maximum stresses were induced on the outer part of the reactor than the inner part.

3.2 Heat Flux Analysis

Figure 5 shows the total heat flux generated in the model. The maximum heat flux of 8.3466e+005 W/m² occurred at the inner chamber of the reactor due to high concentration of the biomass waste and as a result of devolatilization reaction taking place.

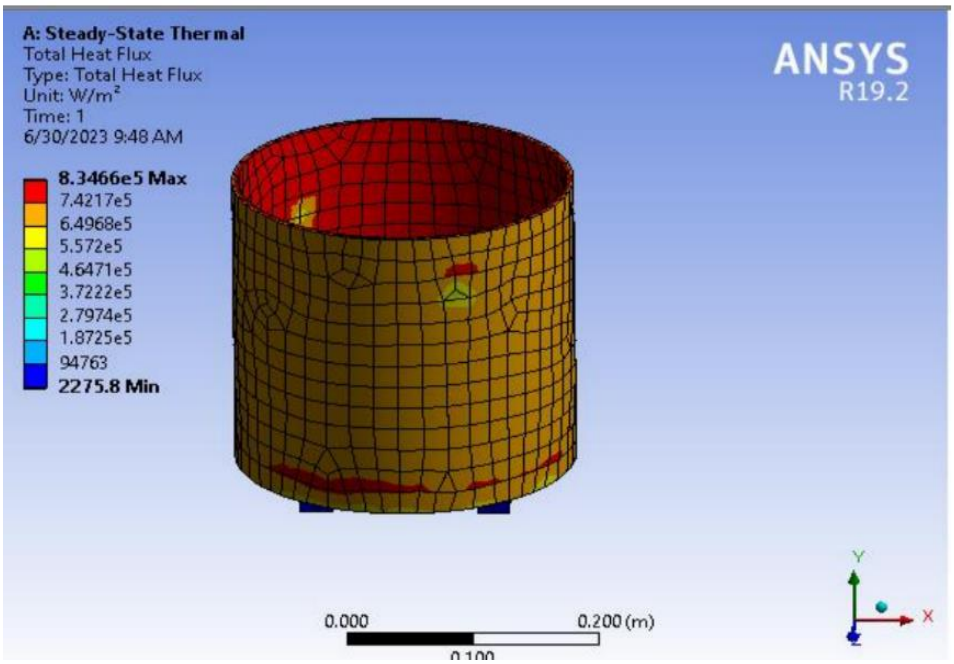

Figure 5: Heat Flux Distribution

The heat flux at the outer part of the reactor chamber was found out to be 6.4968e+005 W/m² and this is less than the heat flux within the reactor as a result of heat being conducted to the inner chamber by conduction mode of heat transfer. The minimum heat flux of 2275.8 W/m² was generated at the reactor stand.

3.3 Static Structural Analysis Result

The static structural analysis simulation was carried out on the reactor model and the equivalent (von-Mises) stress for the reactor model is shown in Figure 6.

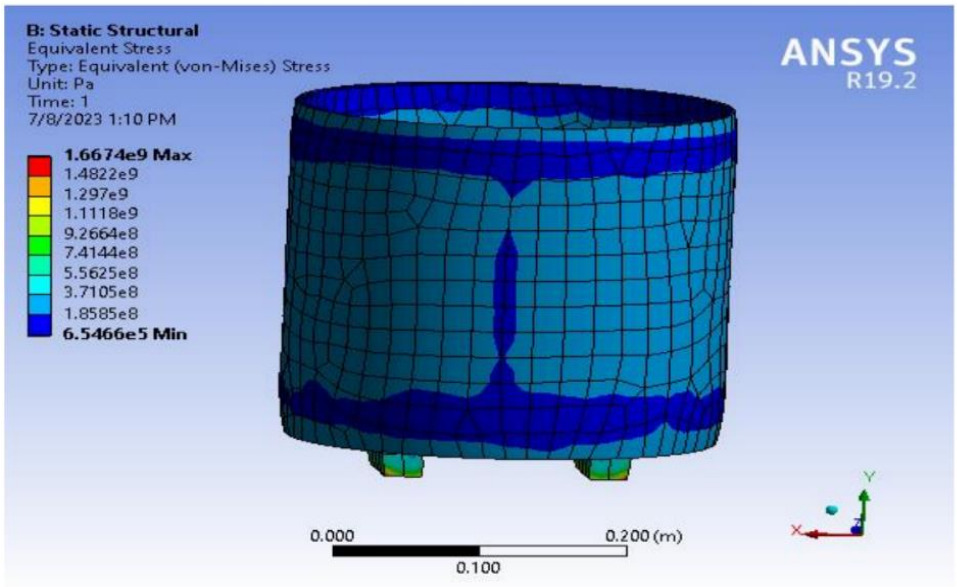

Figure 6: Static Structural Analysis

It was revealed that the maximum equivalent stress the material can withstand at higher temperature is 1.6674e+009 Pa. At the maximum temperature of 550°C, the maximum stress induced at the outer and inner chamber is 1.8585e+008 Pa, which is far lower than the maximum stress the material can withstand without rapture. This means the reactor is safe to operate at temperature higher than 550°C without failure. The minimum stress of 6.5466e+005 Pa was induced at the base of the reactor. The maximum deformation that can occur in the reactor was found to be 1.1093e-003 m and this occur at the flange of the reactor where gas vapour is concentrated as shown in Figure 7. The factor of safety of the reactor is found to be 1 as shown in Figure 8

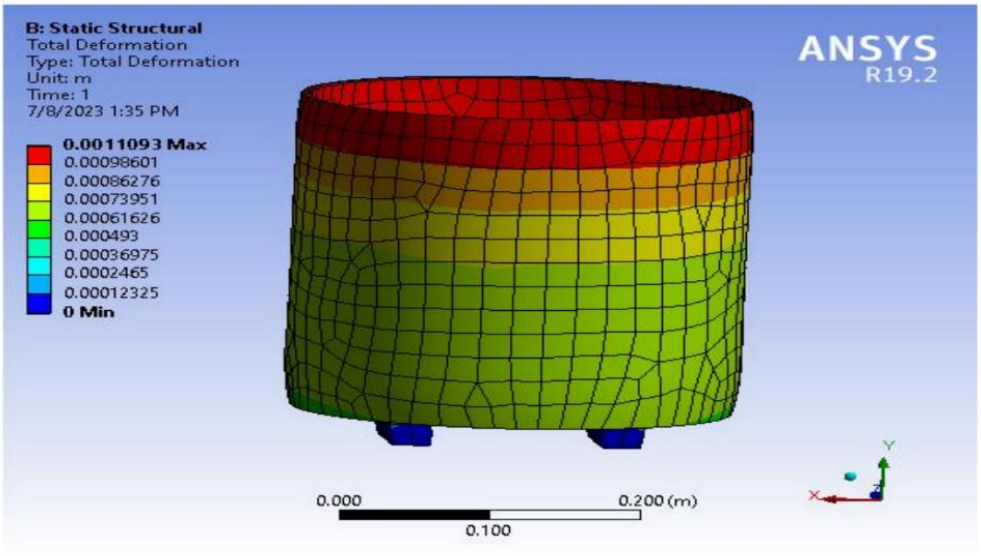

Figure 7: Total Deformation

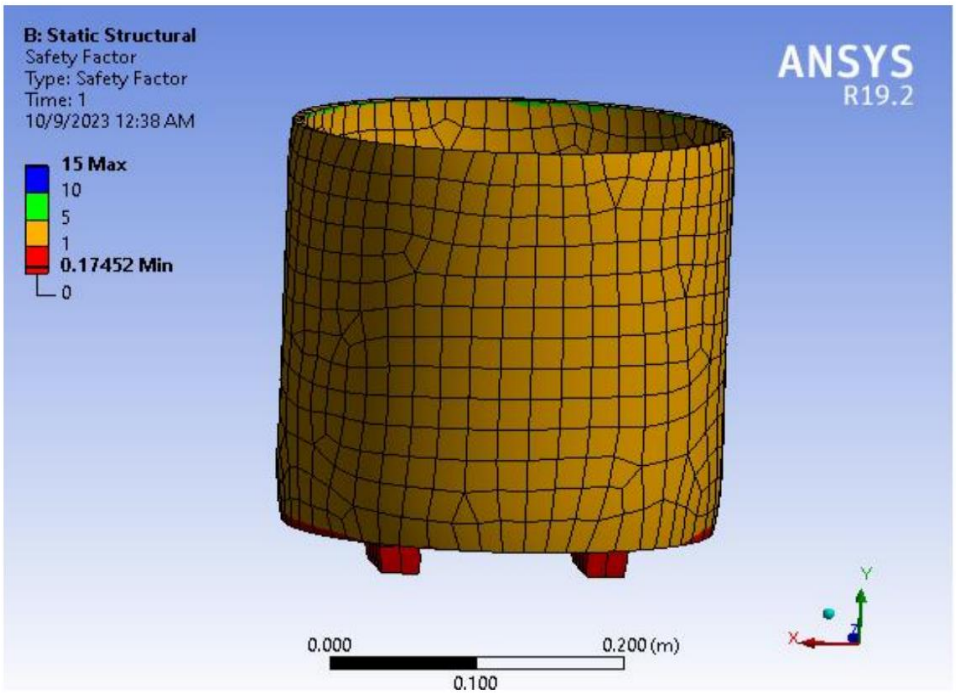

Figure 8: Factor of Safety

4. CONCLUSION

In this study, performance analyses of the reactor were carried out in reference to the steady-state thermal and static structural analysis of the reactor model. The analyses were done using ANSYS Workbench 19. The CFD model was based on mass, momentum, and energy equations for the gaseous phase. 2439 elements compose of 8630 nodes meshes were used to fully capture all the flow details in the reactor. Due to devolatilization reaction of biomass waste, the heat flux generated at 550^{o}C was 8.3466e+005 W/m^{2}, and 1.8585e+008 Pa stress was induced in the reactor. This value is far less than the maximum stress the material can withstand without rupture, and it shows that the material can perform effectively under a high temperature without rupture.

REFERNCES

1. Sivabalan, K., Suhaimi, H., Hamdan, Y., & Jagadeesh, P. (2021). A review on the characteristic of biomass and classification of bioenergy through direct combustion and gasification as an alternative power supply. *Journal of Physics Conf Ser*, 1831, 012033.
2. Khan, S., Paliwal, V., Pandey, V. V., & Kumar, V. (2015). Biomass as Renewable Energy,

International Advanced Research Journal in Science, Engineering, and Technology (IARJSET), 2(1), 301-304.
3. Lebaka, V. (2013). Potential bioresources as future sources of biofuels production: An Overview, in Gupta, V., Tuohy, M. G. (Eds.), *Biofuel Technology* Springer, Berlin, 223-258.
4. Akinola, A. O. (2018). Pyrolysis of cocoa pod husk for bio-char production. *Journal of the Nigerian Institution of Mechanical Engineering*, 8, 141-147.
5. Lima, I. M., Boateng, A. A., & Klasson, K. T. (2009). Pyrolysis of broiler litter: char and product gas characterization. *Industrial and Engineering Chemistry Research*, 48, 1292–1297.
6. Sanchez, C. (2009). Lignocellulosic residues: Biodegradation and bioconversion by fungi. *Biotechnology Advances*, 27(2), 186-194.
7. Sierra, R., Smith, A., & Holtzapple, M. T. (2009). Producing fuels from lignocellulosic biomass. http://72.3.180.220/uploadedFiles/SBE/MemberCenter/0808S10(2).PDF
8. Garcia-Perez, M. (2010). Challenges and Opportunities for Biomass Pyrolysis in Washington State, Washington State Bioenergy Research Symposium, Seattle, November 9-10, 2010.
9. McKendry, P. (2002). Energy production from biomass (part 1): an overview of biomass. *Bioresources Technology*, *83*(1), 37-46.
10. Bain, R. L. (2004): An Introduction to Biomass Thermochemical Conversion, DOE/NASLUGC Biomass and Solar Energy Workshops 3-4, http://www .nrel.gov/docs/gen/fy04/36831e.pdf Hu
11. Aho, A., Kumar, N., Eranen, K., & Murzin, D. Y. (2008). Catalytic pyrolysis of woody biomass in a fluidized bed reactor: influence of the zeolite structure. *Fuel*, 87, 2493-2501.
12. Papadikis, K., Gu, S., Bridgwater, A. V., & Gerhauser, H. (2009). Application of CFD to model fast pyrolysis of biomass. *Fuel Processing Technology*, *90*(4), 504-512.
13. Basu, P. (2018). Biomass Gasification, Pyrolysis and Torrefaction: Practical Design and Theory. 3rd Edition, Academic Press, Elsevier.
14. Uddin, M. N., Techato, K., Taweekun, J., Rahman, M. M., Rasul, M., Mahlia, T. M. I., & Ashrafur, S. M. (2018). An Overview of Recent Developments in Biomass Pyrolysis Technologies, *Energies Review*, 11, 3115-3139
15. Papari, S., & Hawboldt, K. (2015). A review on the pyrolysis of woody biomass to py-oil: Focus on kinetic models. *Renewable and Sustainable Energy Reviews*, 52, 1580-1595.
16. Quesada, L., Pérez, A., Godoy, V., Peula, F. J., Calero, M., & Blázquez, G. (2019). Optimization of the pyrolysis process of a plastic waste to obtain a liquid fuel using different mathematical models. *In Energy Conversion and Management*. Elsevier BV. 188, 19-26. https://doi.org/10.1016/j.enconman.2019.03.054
17. Zhang, M., Zhang, Y., Ma, D., Li, A., Fu, W., Ji, G., & Dong, J. (2022). Numerical investigation on the heat transfer of plastic waste pyrolysis in a rotary furnace. *Chemical Engineering Journal*. Elsevier BV. 41, 445, 136686. https://doi.org/10.1016/j.cej.2022.136686
18. Kumar J. K., Kannan, T. T. M., Chandradass, J., Wilson, D. V. H., & Das, A. (2021). Analysis and simulation of mini pyrolysis reactor for conversion of plastic waste into fuel. *In Materials Today: Proceedings*. Elsevier BV. 45, 7166-7170. https://doi.org/10.1016/j.matpr.2021.02.408,
19. Jhung, J. M. (2012). Fatigue Analysis of a Reactor Pressure Vessel for SMART. *Nuclear Engineering and Technology*, *44*(6), 683-688.
20. Mellin, P., Kantarelis, E., & Yang, W. (2014). Computational fluid dynamics modeling of biomass fast pyrolysis in a fluidized bed reactor, using a comprehensive chemistry scheme. *Fuel*, 117(A), 704–715.
21. Xue, Q., Dalluge, D., Heindel, T., Fox, R., & Brown, R. (2012). Experimental validation and CFD modeling study of biomass fast pyrolysis in fluidized-bed reactors. *Fuel*, 97, 757-769.
22. Wijayanti, W., Musyaroh, Sasongko, M. N., Kusumastuti, R., & Sasmoko. (2021). Modelling analysis of pyrolysis process with thermal effects by using Comsol Multiphysics. In Case Studies in Thermal Engineering. Elsevier BV. 28, 101625. https://doi.org/10.1016/j.csite.2021.101625
23. Solanki, S., Baruah, B., & Tiwari, P. (2022). Modeling and simulation of wood pyrolysis process using COMSOL Multiphysics. *In Bioresource Technology Reports*. Elsevier BV. 17, 100941. https://doi.org/10.1016/j.biteb.2021.100941
24. Yoon, J., Kim, Y., & Song, H. (2020). Numerical and experimental analysis of thermal-flow characteristics in a pyrolysis reactor of a gas scrubber designed based on similitude theory, *Journal of the Air & Waste Management Association*. DOI: 10.1080/10962247.2020.1738283
25. Yu, P. (2020). Modelling and Simulation of Reactor Pressure Vessel Failure during Severe Accidents. Doctoral Thesis Submitted to Department of Physics, School of Engineering Science, KTH Royal Institute of Technology, Shekholm, Sweden.

